DALTON
FULL PAPER

Luminescent gold(I) macrocycles with diphosphine and 4,4′-bipyridyl ligands

Marie-Claude Brandys, Michael C. Jennings and Richard J. Puddephatt *

Department of Chemistry, University of Western Ontario, London, N6A 5B7, Canada

Received 30th June 2000, Accepted 10th October 2000
First published as an Advance Article on the web 1st December 2000

The complexes $[\{-Ph_2P(CH_2)_nPPh_2AuNC_5H_4C_5H_4NAu-\}_x]^{2x+}$ $[CF_3CO_2^-]_{2x}$ (n = 1–6) were prepared as colourless, air-stable solids by reaction of silver trifluoroacetate with the corresponding precursor complex $[(CH_2)_n(Ph_2PAuCl)_2]$, and subsequent treatment of the products $[(CH_2)_n(Ph_2PAuO_2CCF_3)_2]$ with 4,4′-bipyridyl. The complexes are suggested to exist in solution as an equilibrium mixture of linear oligomers and cyclic complexes. When n = 1, 3 or 5 the cationic complexes were shown to exist as 26-, 30- and 34-membered macrocyclic rings respectively; only when n = 1 are there significant intramolecular Au · · · Au contacts of 3.106(1) and 3.084(1) Å. Some of the complexes are strongly emissive at room temperature in solution and in the solid state.

Introduction

There is growing interest in the synthesis of gold(I) complexes with macrocyclic, oligomeric or polymeric structures.[1] The construction of unusual molecular architectures is aided by the tendency of gold(I) to form linear, 2-coordinate complexes that may then undergo additional weaker gold–gold attractions. Experimental and theoretical studies indicate that these aurophilic interactions with distances from 2.5 to 4 Å may give bonding forces of *ca.* 30 kJ mol^{-1}, comparable to hydrogen bonding forces. As with hydrogen bonding in organic chemistry, the aurophilic attractions can lead to unique molecular conformations, stereochemistry, crystal packing and physical properties in gold chemistry.[1–8] If the gold(I) centres are bonded to bidentate ligands, polymers or rings may be formed, and the Au · · · Au interactions can determine the favoured structure.[9] For example, in cationic complexes containing diphosphine and *trans*-bis(pyridyl)ethylene ligands, the occurrence of a crossover from ring to polymer was demonstrated for the complexes illustrated in Scheme 1. In solution, the lability of the N-donor ligand allowed easy equilibration between rings and oligomers and the orderly build-up of crystalline rings or polymers was possible in some cases. The conformations of the polymers were determined by the nature of the diphosphine ligands as indicated in Scheme 1.[9]

This article describes an investigation of new gold(I)-containing oligomers or macrocycles using 4,4′-bipyridyl as the rigid-rod, bidentate N-donor ligand. The aim was to search for similarities and differences compared to the chemistry of the *trans*-bis(pyridyl)ethylene ligands used previously (Scheme 1).[9] The photoluminescence behaviour of the products was also studied and molecular modeling was performed in an attempt to rationalize the conformations adopted.

Results

The complexes $[(CH_2)_n(Ph_2PAuCl)_2]$ **2**–**7** (n = 1–6), were prepared as colourless, air-stable products by treating two equivalents of $[AuCl(SMe_2)]$, **1**, with the corresponding diphosphine ligand in acetone at room temperature.[10–15] The ^{31}P and ^{1}H NMR data can be found in Table 1. Addition of silver trifluoroacetate to a suspension of **2**–**7** in tetrahydrofuran results in formation of silver chloride and the corresponding soluble bis(trifluoroacetate) complexes, as described in Scheme 2. These

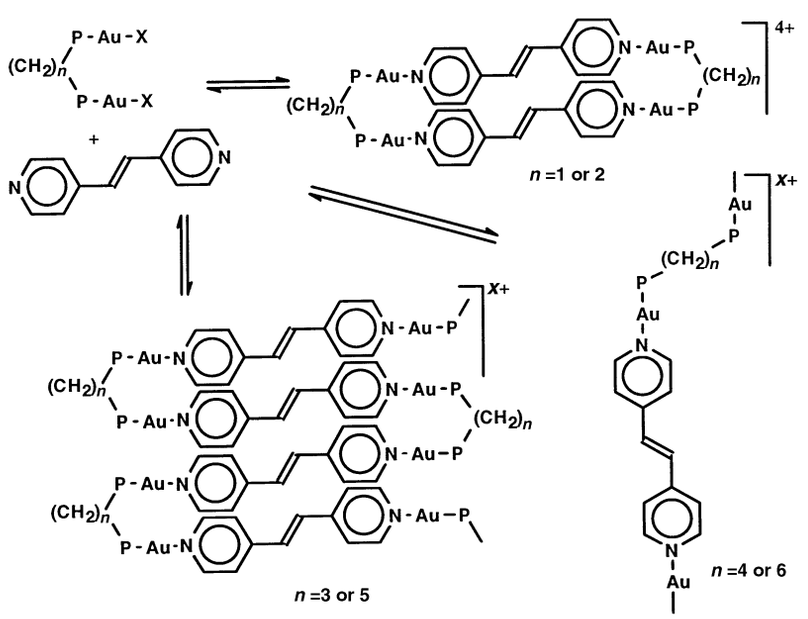

Scheme 1 X = CF_3CO_2, P = PPh_2.

Table 1 Comparison of ^{31}P and ^{1}H NMR data for complexes **2**–**13**

Complex	$\delta(^{31}P)$	$\delta(CH_2P)$	$\delta(CH_2CH_2P)$
2, **8**	24.25, 25.59	3.60, 4.40	—
3, **9**	32.12, 26.75	2.62, 2.80	—
4, **10**	27.02, 21.70	2.80, 2.94	1.91, 1.95
5, **11**	29.92, 24.70	2.45, 2.50	1.80, 1.83
6, **12**	29.52, 24.29	2.42, 2.49	1.67, 1.66
7, **13**	29.98, 24.22	2.37, 2.48	1.56, 1.55

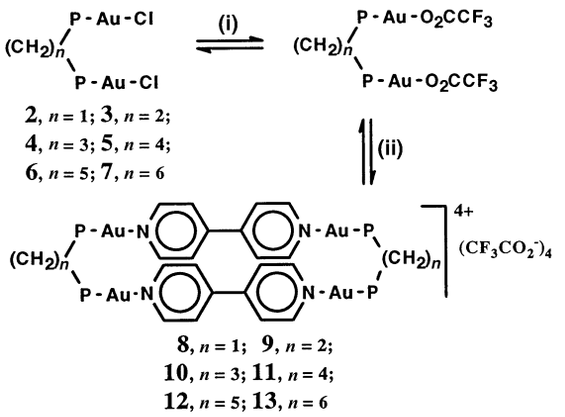

Scheme 2 P = PPh_2. Reagents: (i) AgO_2CCF_3, −AgCl; (ii) 4,4′-bipyridine.

complexes were not isolated, but their solutions were filtered to remove silver chloride then treated with 4,4′-bipyridine to give the cationic complexes $[\{Ph_2P(CH_2)_nPPh_2AuNC_5H_4C_5H_4NAu\}_x]^{2x+}[CF_3CO_2^-]_{2x}$ **8**–**13** (n = 1–6) by displacement of the weakly coordinated trifluoroacetate ligands. These complexes are colourless, air-stable solids but they are light sensitive and were stored in the dark. They are slightly soluble in chloroform and dichloromethane, and were characterized in solution by NMR spectroscopy. The isolated complexes gave satisfactory analytical data, and study by thermogravimetric analysis indicated that each decomposed over a temperature range from 170 to 245 °C to leave a residue of metallic gold.

The key question for the new complexes is whether they exist as rings or chains or as an equilibrium mixture of both (Scheme 3). The room temperature ^{31}P NMR spectra of **8**–**13** contain only a singlet, indicating effective equivalence of all phosphorus atoms. In addition, single resonances were observed in the ^{1}H NMR spectra for each of the bipyridyl protons *ortho* and *meta* with respect to nitrogen, and for

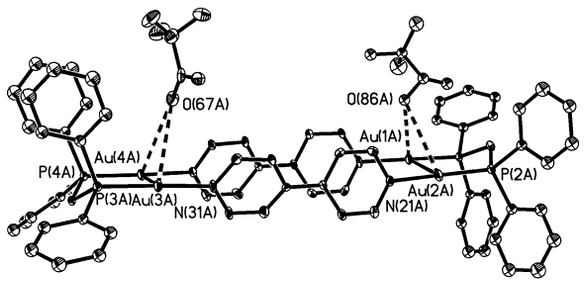

Fig. 1 A view of the structure of complex **8**. Two distant trifluoroacetate ions are not shown.

each type of methylene group for the diphosphine ligands. A compilation of the NMR data can be found in Table 1. The data are consistent either with formation of symmetrical ring complexes in each case or with very rapid equilibration between ring and chain structures, probably by easy reversible displacement of bipyridine nitrogen donors from gold(I) by trifluoroacetate.[9]

Molecular structures of the macrocycles $[\{-Ph_2P(CH_2)_nPPh_2AuNC_5H_4C_5H_4NAu-\}_2]^{4+}[CF_3CO_2^-]_4$, n = 1, 8; n = 3, 10; n = 5, 12

Many attempts were made to grow crystals of the complexes **8**–**13**. Finally crystals were grown for **8**, **10** and **12** (n = 1, 3 and 5 respectively) from concentrated solutions of dichloromethane layered with pentane, but no single crystals for **9**, **11** and **13** (n = 2, 4 and 6 respectively) suitable for single crystal X-ray analysis could be grown. The structures of **8**, **10** and **12** allow comparison of structures with different lengths of spacer groups between the two phosphorus donors of the diphosphine ligands.

Fig. 1 illustrates the molecular structure of the cationic macrocycle $[\{-Ph_2PCH_2PPh_2AuNC_5H_4C_5H_4NAu-\}_2]^{4+}$ in complex **8**, while Tables 2 and 3 contain selected bond lengths and angles. The complex adopts a macrocyclic structure and the geometry about each gold(I) centre is approximately linear, with angles N(11)–Au(1)–P(1), N(21)–Au(2)–P(2), N(31)–Au(3)–P(3) and N(41)–Au(4)–P(4) of 175.4(3), 176.7(3)°, 177.4(4) and 175.1(3)° respectively. Fig. 1 features a 26-membered ring with four gold(I) atoms. The transannular gold–gold distances are Au(1)–Au(2) 3.1061(8) and Au(3)–Au(4) 3.0841(8) Å, indicating a significant aurophilic interaction, and the similar spacing between roughly parallel pyridyl groups allows a π- stacking attraction also.[1–8]

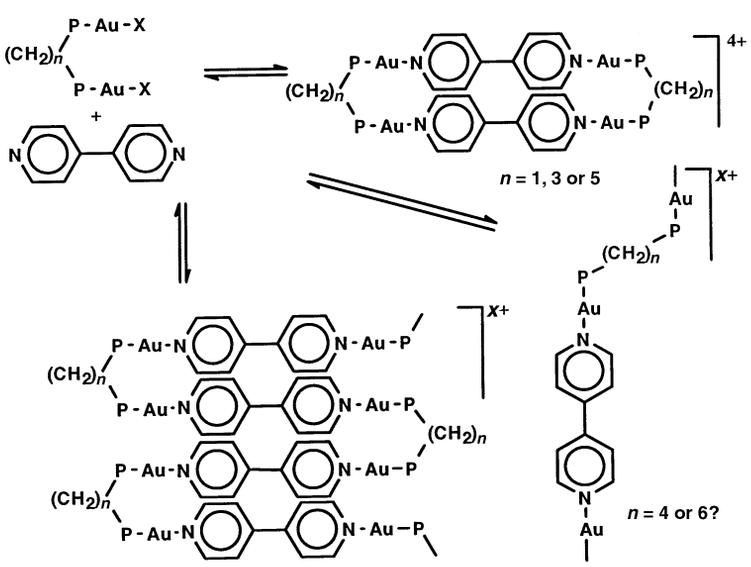

Scheme 3 P = PPh_2.

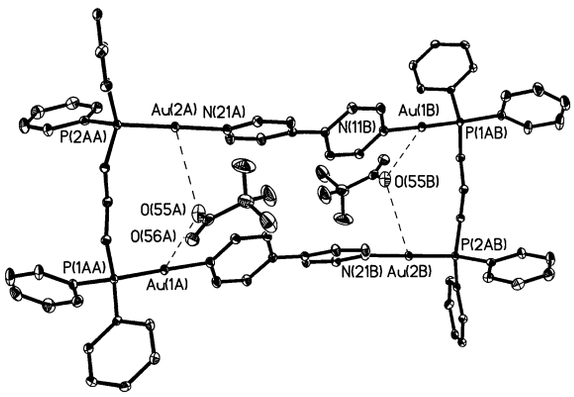

Fig. 2 A view of the structure of the cation **10**. Two distant trifluoroacetate ions are not shown.

Table 2 Selected bond lengths [Å] and angles [°] for complex **8**

Au(1)–N(11)	2.098(9)	Au(3)–N(31)	2.044(10)
Au(1)–P(1)	2.230(3)	Au(3)–P(3)	2.241(3)
Au(1)–Au(2)	3.1061(8)	Au(3)–Au(4)	3.0841(8)
Au(2)–N(21)	2.075(10)	Au(4)–N(41)	2.107(10)
Au(2)–P(2)	2.236(3)	Au(4)–P(4)	2.232(3)
N(11)–Au(1)–P(1)	175.4(3)	N(31)–Au(3)–P(3)	177.4(4)
N(21)–Au(2)–P(2)	176.7(3)	N(41)–Au(4)–P(4)	175.1(3)

Table 3 Selected bond lengths [Å] and angles [°] for complex **10**

Au(1)–N(11)	2.084(6)	Au(2)–N(21)	2.081(6)
Au(1)–P(1)	2.240(2)	Au(2)–P(2)	2.240(2)
N(11)–Au(1)–P(1)	178.2(2)	N(21)–Au(2)–P(2)	178.3(2)

A view of the structure of the cation $[\{-Ph_2P(CH_2)_3PPh_2AuNC_5H_4C_5H_4NAu-\}_2]^{4+}$ in complex **10** is shown in Fig. 2, and selected bond lengths and angles are listed in Table 3. The geometry about the gold(I) center is linear with angles N(11)–Au(1)–P(1) and N(21)–Au(2)–P(2) of 178.2(2) and 178.3(2)° respectively and the complex adopts a macrocyclic structure, containing a 30-membered ring with four gold(I) atoms. There is a crystallographic centre of symmetry at the ring centre. The intramolecular gold–gold distance, Au(1)···Au(2) 5.279(1) Å, lies well outside the range for a bonding interaction.[1–9] For each ring there are four trifluoroacetate counter ions and two of these are partly enclosed in the macrocyclic ring, as shown in Fig. 2, this being aided by twisting of the bridging bipy ligand to create a suitable cavity. The twist of the 4,4′-bipyridyl ligand in **10** (Fig. 2) is clearly greater than in **8** (Fig. 1). The shortest Au···O contacts in **10** are Au(1)···O(55) 3.05(1) and Au(2)···O(55) 3.37(1) Å; this is probably best considered a weak ionic attraction between the cation and anion.

A view of the molecular structure of the cation $[-\{Ph_2P(CH_2)_5PPh_2AuNC_5H_4C_5H_4NAu-\}_2]^{4+}$ in complex **12** is shown in Fig. 3(a), as determined by a partial structure determination. The crystals were of poor quality but the data sufficient to determine the structure of the cation. The intramolecular gold–gold distances, the longest being Au(1)···Au(3) 8.05(1) Å, are clearly non-bonding, as expected with the long $(CH_2)_5$ bridges between phosphorus donors. There is disorder in the position of Au(4) and so there are two values of the distance Au(2)···Au(4) of 6.82(2) and 7.24(2) Å, both of which are significantly shorter than the Au(1)···Au(3) distance. There is also resolved disorder in the position of P(4) but, though the lighter atoms in this region [especially C(10) and the pyridyl ring containing N(41)] must also be disordered, this was not resolved and so bond distances are not discussed. The complex contains an unsymmetrical 34-membered ring with four gold(I) atoms. There is a large cavity within the ring, but only one

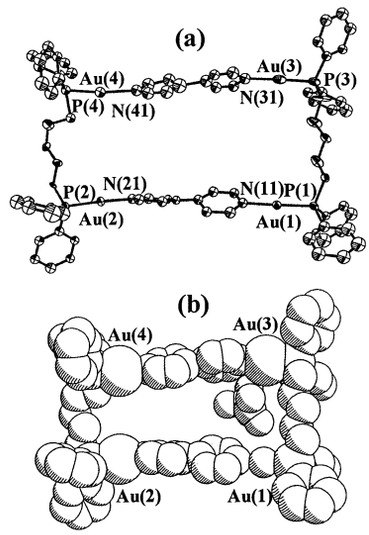

Fig. 3 (a) A view of the structure of the cation **12**. The disordered trifluoroacetate ions are not shown and only the major component of the disordered Au(4) and P(4) atoms is shown. Bond distances (Å) : Au(1)–P(1) 2.245(9); Au(2)–P(2) 2.249(8); Au(3)–P(3) 2.22(1); Au(4)–P(4) 2.18(3). (b) A space filling model showing the partial encapsulation of one trifluoroacetate anion, weakly bonded to Au(3) with d(Au3···O86) = 3.16(4) Å.

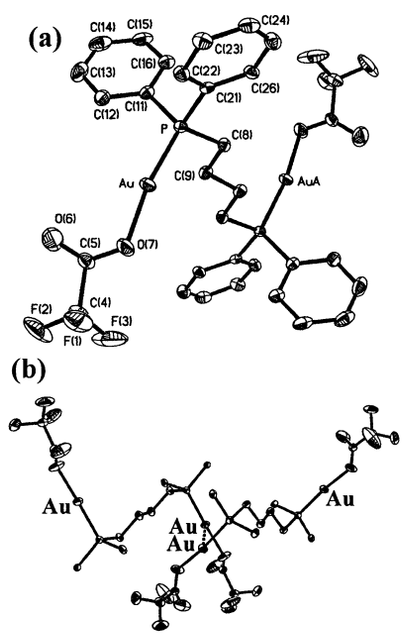

Fig. 4 (a) A view of the structure of the complex **14**. (b) A part of the one-dimensional chain structure formed by intermolecular Au···Au bonding.

trifluoroacetate anion is partly enclosed (Fig. 3b), and it is possible that the inefficient solid state packing leads to the observed poor crystal quality. The increase in the ring cavity size with increasing number of methylene spacer groups in the diphosphine ligand is clear by comparison of Figs. 1–3.

In one attempt to grow crystals of complex **11**, crystals of the parent trifluoroacetate complex **14** were obtained. The structure is shown in Fig. 4, and bond parameters are listed in Table 4. The molecules exist in the *anti* conformation, such that there is a center of symmetry at the midpoint of the C(9)–C(9′) bond (Fig. 4a). If this conformation is also preferred in the bipyridine complex it would of course lead to a polymeric rather than cyclic structure. The complex forms one-dimensional chains in the solid state through weak intermolecular Au···Au bonding (Fig. 4b) with d(Au···Au) = 3.584(1) Å. The structure is similar to that of the iodide derivative $[IAuPPh_2CH_2CH_2-$

Table 4 Selected bond lengths [Å] and angles [°] for complex **14**

Au–O(7)	2.081(9)	C(5)–O(7)	1.18(1)
Au–P	2.214(3)	C(5)–O(6)	1.19(2)
C(4)–C(5)	1.51(2)		
O(7)–Au–P	171.0(3)	C(5)–O(7)–Au	123.8(9)
O(7)–C(5)–O(6)	128(1)		

Table 5 Energies and transannular Au · · · Au distances in complexes **8**–**13**, as predicted by molecular mechanics calculations[a]

Complex	E/kcal mol^{-1}	d(Au · · · Au)/Å
8	−18	3.4
9	26	5.6
10	−10	5.7
11	25	5.9
12	−1	6.1
13	25	6.6

[a] The PAuN bond was constrained to be linear. No anions were present in the MM calculations.

$CH_2CH_2PPh_2AuI$], but this has a shorter intermolecular contact d(Au · · · Au) = 3.148(1) Å, probably due to the presence of the softer iodide ligand that enhances the aurophilic attraction.[8]

Molecular modeling

Molecular mechanics calculations were carried out for the cations in complexes **8**–**13**, in the macrocyclic ring form, and data are listed in Table 5. The trend in calculated energies is that the ring structures are more favored for the diphosphine ligands $(CH_2)_n(PPh_2)_2$, when n = 1, 3 or 5 compared to when n = 2, 4 or 6. This is presumably because the *syn* conformation of the diphosphine required for macrocycle formation is more favorable with n odd, since the CH_2 groups can then have the staggered conformation with respect to each other. It is suggested that there is a higher relative concentration of non-cyclic oligomers, with the diphosphines in the *anti* conformation as established in complex **14**, in solution in the cases with n = 2, 4 and 6 and that this may be at least a partial reason for our inability to crystallize these compounds, despite many attempts.

Table 5 also gives the mean Au · · · Au separation for the complexes. It overestimates the value when n = 1, probably because there are no parameters for the transannular Au · · · Au attraction incorporated in the model. It underestimates the value of d(Au · · · Au) when n = 5, but the energy differences with varying Au · · · Au separation are small in this case, and it is likely that anion inclusion (Fig. 3b) leads to the higher value of d(Au · · · Au) observed in the solid state structure of **12**.

Photoluminescence studies

The emission spectra of complexes **8**–**13** at room temperature were studied both in the solid state as KBr disks and in solution in dichloromethane and data are listed in Table 6. In the solid state **8**, **10**, **12** and **13** gave only a very broad, weak emission in the region 420–440 nm. However, **9** and **11** give strong emission with well defined structure as illustrated in Fig. 5 for **9**. The approximate energy difference between neighboring bands for both **9** and **11** was 1330 cm^{-1}. This splitting is similar to that observed for ligand based π–π* transitions for bipyridine derivatives, but it should be noted that 4,4′-bipyridine is not emissive at room temperature and its protonated form displays weak emission so a pure π–π* transition is not expected to lead to room temperature emission.[16] This factor indicates that the emission is strongly affected by the presence of the gold(I) centres and may indicate that the excitation has considerable d(Au)–π*(bipy) character. The featureless solution emission, combined with the observation of a significant red shift from solution to solid state emission[1,17] (Table 6, Fig. 5), suggests

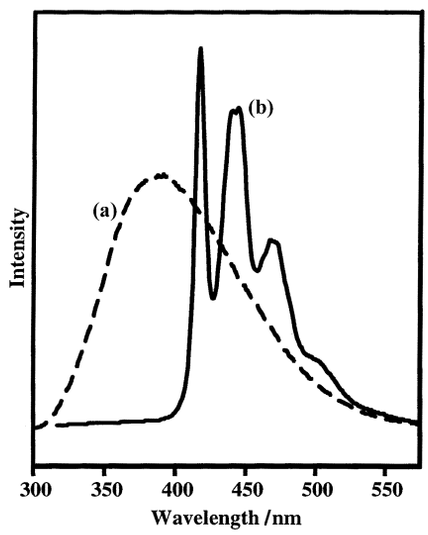

Fig. 5 The room temperature emission spectra of complex **9**: (a) in dichloromethane solution with λ_{ex} = 254 nm and (b) in a solid KBr disk with λ_{ex} = 300 nm.

Table 6 Emission spectral data (nm) of the complexes in dichloromethane solution or in the solid state as KBr disks

Complex	Solution excitation	Solution emission	Solid excitation	Solid emission
8	265, 350	390[a]	355	430[b,c]
9	270, 330	390[d]	305	417, 440, 468, 500[e]
10	265, 340	410[c]	288, 378[b]	420[b,f]
11	265, 325	385[d]	300	416, 440, 470, 500[e]
12	265, 330	395[g]	265, 360[b]	420[b,e]
13	265, 330	395[g]	279, 360[b]	440[b,e]

Approximate excitation energies are given for maximum emission intensity; the emission energies are not significantly affected by changing λ_{ex}. [a] λ_{ex} = 267 nm. [b] The emission was very weak and broad in these cases. [c] λ_{ex} = 340 nm. [d] λ_{ex} = 254 nm. [e] λ_{ex} = 300 nm. [f] λ_{ex} = 288 nm. [g] λ_{ex} = 330 nm.

that the solution state emission can be assigned to a gold-centred 5d–6p excited state. Since the 6p(Au) and π*(bipy) orbitals can mix, a different combination may be involved for the solution and solid state emissions.

Complexes **8**–**13** in dichloromethane solution each give a single emission band, with the peak maximum ranging from 390 to 410 nm, as illustrated in Fig. 5 for complex **9**. For all complexes there was a red shift on going from solution to the solid state (Table 6). This is a common effect in the emission spectra of gold(I) complexes,[17] and can be attributed to the presence of intermolecular Au · · · Au interactions or association through π–stacking effects.

Discussion

Each complex **8**, **10** and **12** contains the expected linear, two-coordinate gold(I) centres, with each gold atom bound to a nitrogen atom and a phosphorus atom of the bridging 4,4′-bipyridyl (bipy) and diphosphine ligand respectively. It is interesting to compare the macrocyclic structures observed in this work with the structures found for the corresponding complexes with the bridging ligand *trans*-1,2-bis(4-pyridyl)ethylene (bipyen) studied previously.[9a] A summary is given in Table 7.

With the ligand bipyen the structures were rationalized in terms of the effects of Au · · · Au bonding. Thus, for the diphosphines $Ph_2P(CH_2)_nPPh_2$ with n = 1 or 2, the ring structures naturally contain interannular Au · · · Au distances short enough to give a significant aurophilic attraction and this gave a thermodynamic preference for ring formation (Table 7). When n > 2 this effect was not present and polymeric structures, in

Table 7 Summary of the structures of complexes $[\{Ph_2P(CH_2)_n PPh_2AuNNAu\}_x]^{2x+}$, as a function of the number of methylene groups *n* and nature of the bridging ligand NN = bipy (bipyridine) or bipyen

	x, *y*[a]		
n	bipy	bipyen	*d*(Au · · · Au)[b]/Å
1	Ring, 2, 26	Ring, 2, 28	3.1
2	?	Ring, 2, 30	3.6
3	Ring, 2, 30	Polymer, ∞	5.3
4	?	Polymer, ∞	
5	Ring, 2, 34	Polymer, ∞	7.6
6	?	Polymer, ∞	

[a] *y* = Ring size when *x* = 2; ? indicates not known. [b] Approximate average transannular Au · · · Au separation in the ring structures only.

which the diphosphine could have either the *syn* (*n* = 3 or 5) or *anti* (*n* = 4 or 6) conformation, were observed.[9] For example, when *n* = 3, a sinusoidal polymer was formed with closest gold–gold contact of 5.98(1) Å, which is much too long to allow any bonding to occur. In contrast, complex **10** has the ring structure even though the transannular Au · · · Au distance of 5.279(1) Å is clearly non-bonding. In both complexes the diphosphine adopts the *syn* conformation. Similarly, when *n* = 5, the complex with bipyen is a sinusoidal polymer but with bipy the solid state structure is the macrocyclic **12**, although with *syn* conformation of the diphosphine in both cases. Why are different structures obtained? First, it should be emphasized that there is likely to be a fast equilibrium between structural forms in solution and so the form that crystallizes may not be the only, or even the major, complex present. There will be a tendency for the least soluble form present to crystallize, and so any discussion based on electronic/steric effects may not be valid. The main differences between bipy and bipyen are the distance between the nitrogen donors (longer for bipyen) and the tendency to twist from planarity (greater for bipy), but it is not obvious that either effect would greatly influence the relative stabilities of cyclic *versus* chain structures. The twisting of the bipy ligand might affect π-stacking in the macrocycles, but this is not evident in the structures of **10** and **12**.

The fact that the macrocyclic complexes **8**, **10** and **12** could be crystallized and are not luminescent, whereas **9** and **11** are emissive but do not crystallize well, might suggest that different structures are adopted and that **9** and **11** may have polymeric structures in the solid state. This explanation could not be confirmed crystallographically, but the molecular modeling calculations do lend support to the hypothesis. In addition, known polymeric gold(I) complexes are much more weakly emissive than molecular analogues.[1]

Experimental

NMR spectra were recorded using a Gemini 300 MHz spectrometer. ^{1}H and ^{31}P chemical shifts are reported relative to TMS and 85% H_3PO_4 respectively. Thermogravimetric analyses were performed using a Perkin-Elmer Series 7 TGA instrument at a heating rate of 20 °C min^{-1} on samples of 10 to 40 mg under nitrogen. Molecular modeling experiments were performed using the CAChe Scientific software package.[18] Emission spectra were recorded by using a Fluorolog-3 (ISA Jobin Yvon-Spex) spectrofluorimeter. Typically, a 1 nm slit width was used for solid samples and a 3 nm slit width for solution samples in quartz cuvettes.

Preparations

$[AuCl(SMe_2)]$, 1. This procedure is modified from the literature method.[10] Au (9.88 g, 50.2 mmol) was dissolved in boiling *aqua regia* (160 mL). The volume was reduced to *ca*. 30 mL by boiling, then HCl (*ca*. 100 mL, conc.) was added, and the volume again reduced to *ca*. 30 mL. This procedure was repeated until the vapors produced were no longer brown. The final solution (30 mL) was cooled to room temperature and methanol (*ca.* 200 mL) added. With minimum light exposure, SMe_2 (*ca*. 10 mL, excess) was added dropwise, with continuous stirring, until no red colour appeared. The white precipitate of the product was recovered by filtration, washed with methanol, diethyl ether and pentane and dried under vacuum. Yield: 13.8 g (93%). NMR in acetone-d_6: δ(^{1}H) 2.86 [s, 6H, CH_3].

$[CH_2(Ph_2PAuCl)_2]$, 2. A solution of dppm (0.083 g, 0.215 mmol) in acetone (15 mL) was added to a suspension of $[AuCl(SMe)_2]$ (0.127 g, 0.430 mmol) in acetone (25 mL). The mixture was stirred for 2 h, to give a white precipitate, which was collected by filtration, washed with acetone, diethyl ether and pentane, and dried under vacuum. Yield: 0.16 g (89%). Similarly prepared were $[(CH_2)_2(Ph_2PAuCl)_2]$, **3**, yield 76%; $[(CH_2)_3(Ph_2PAuCl)_2]$, **4**, yield 84%; $[(CH_2)_4(Ph_2PAuCl)_2]$, **5**, yield 85%; $[(CH_2)_5(Ph_2PAuCl)_2]$, **6**, yield 92%; $[(CH_2)_6(Ph_2PAuCl)_2]$, **7**, yield 90%. The complexes were characterized by comparison of the NMR data with literature values.[10–15]

$[\{-Ph_2PCH_2PPh_2AuNC_5H_4C_5H_4NAu-\}_2]^{4+}$ $[CF_3CO_2^-]_4$, 8. Silver trifluoroacetate (0.057 g, 0.257 mmol) was added to a suspension of $[(CH_2)(Ph_2PAuCl)_2]$ (0.108 g, 0.128 mmol) in THF (15 mL). The mixture was stirred for 45 min, then filtered through Celite into a flask containing a solution of 4,4′-bipyridyl (0.0106 g, 0.0679 mmol) in THF (25 mL). After 1 h, the white solid product was collected by filtration, washed with THF, acetone, diethyl ether and pentane and dried under vacuum. Yield: 0.11 g (72%). Calc. for $C_{39}H_{30}Au_2F_6N_2O_4P_2$: C, 40.34; H, 2.61; N, 2.41. Found: C, 39.03; H, 2.56; N, 2.21%. NMR in $CDCl_3$: δ(^{1}H) 9.04 [m, 4H, *o*-H py]; 7.47–7.36 [m, 28H, *m*-H py + Ph]; 4.40 [m, 2H, CH_2P]; δ(^{31}P) 25.59 (s). TGA: Au yield 35.2% (found), 33.94% (calc.); decomposition onset 245 °C.

The following complexes were prepared similarly.

$[\{-Ph_2P(CH_2)_2PPh_2AuNC_5H_4C_5H_4NAu-\}_x]^{2x+}$ $[CF_3CO_2^-]_{2x}$, 9. From $[(CH_2)_2(Ph_2PAuCl)_2]$ (0.327 g, 0.379 mmol). Yield : 0.35 g (80%). Calc. for $C_{20}H_{16}AuF_3NO_2P$: C, 40.90; H, 2.75; N, 2.39. Found: C, 40.53; H, 2.65; N, 2.44%. NMR in $CDCl_3$: δ(^{1}H) 8.81 (m, 4H, *o*-H py); 7.71–7.51 (m, 24H, *m*-H py + Ph); 2.80 (m, 4H,CH_2P); δ(^{31}P) 26.75 (s). TGA: Au yield 34.0% (found), 33.5% (calc.); decomposition onset 245 °C.

$[\{-Ph_2P(CH_2)_3PPh_2AuNC_5H_4C_5H_4NAu-\}_2]^{4+}$ $4[CF_3CO_2^-]$, 10. From $[(CH_2)_3(Ph_2PAuCl)_2]$ (0.1052 g, 0.1199 mmol). Yield: 0.11 g (76%). Calc. for $C_{41}H_{34}Au_2F_6N_2O_4P_2$: C, 41.42; H, 2.89; N, 2.36. Found: C, 41.43; H, 2.85; N, 2.07%. NMR in $CDCl_3$: δ(^{1}H) 8.80 [m, 4H, *o*-H py]. TGA: Au yield 33.2% (found), 33.1% (calc.); decomposition onset 231 °C.

$[\{-Ph_2P(CH_2)_4PPh_2AuNC_5H_4C_5H_4NAu-\}_x]^{2x+}$ $[CF_3CO_2^-]_{2x}$, 11. From $[(CH_2)_4(Ph_2PAuCl)_2]$ (0.109 g, 0.123 mmol). Yield: 0.10 g (64%). Calc. for $C_{21}H_{18}AuF_3NO_2P$: C, 41.94; H, 3.02; N, 2.33. Found: C, 40.52; H, 3.09; N, 2.32%. NMR in $CDCl_3$: δ(^{1}H) 8.77 (m, 4H, *o*-H py). TGA: Au yield 33.1% (found), 32.8% (calc.); decomposition onset 212 °C.

$[\{-Ph_2P(CH_2)_5PPh_2AuNC_5H_4C_5H_4NAu-\}_2]^{4+}$ $4[CF_3CO_2^-]$, 12. From $[(CH_2)_5(Ph_2PAuCl)_2]$ (0.164 g, 0.181 mmol). Yield: 0.05 g (64%). Calc. for $C_{43}H_{38}Au_2F_6N_2O_4P_2$: C, 42.43; H, 3.15; N, 2.30. Found: C, 41.57; H, 3.20; N, 2.30%. NMR in $CDCl_3$: δ(^{1}H) 8.80 [m, 4H, *o*-H py]. TGA: Au yield 35.0% (found), 32.4% (calc.); decomposition onset 171 °C.

$[\{-Ph_2P(CH_2)_6PPh_2AuNC_5H_4C_5H_4NAu-\}_x]^{2x+}$ $[CF_3CO_2^-]_{2x}$, 13. From $[(CH_2)_6(Ph_2PAuCl)_2]$ (0.171 g, 0.186 mmol). Yield: 0.05 g (60%). Calc. for $C_{22}H_{20}AuF_3NO_2P$: C, 42.92; H, 3.28; N, 2.28. Found: C, 42.19; H, 3.28; N, 2.24%. NMR in $CDCl_3$: δ(^{1}H) 8.82 [m, 4H, *o*-H py]. TGA: Au yield 32.9% (found), 32.0% (calc.); decomposition onset 202 °C.

Table 8 Crystal data and structure refinements for complexes **8**, **10**, **12** and **14**

	8	**10**	**12**[a]	**14**
Formula	$C_{79}H_{62}Au_4Cl_2F_{12}N_4O_8P_4$	$C_{44}H_{41}Au_2ClF_6N_2O_4P_2$	$C_{84}H_{76}Au_4F_9N_4O_6P_4$	$C_{32}H_{28}Au_2F_6O_4P_2$
M	2405.97	1267.11	2320.23	1046.42
T/K	150	150	200	200
Crystal system	Orthorhombic	Monoclinic	Orthorhombic	monoclinic
Space group	*Pna*2(1)	$P2_1/n$	*Iba*2	*C*2/*c*
a/Å	26.5731(7)	13.2510(2)	17.3326(12)	21.4364(7)
b/Å	18.7220(3)	19.1399(5)	23.8685(13)	13.2988(5)
c/Å	16.8531(4)	18.1822(4)	48.0435(18)	13.2773(6)
β/°	—	105.789(2)	—	117.081(2)
V/Å^3	8384.4(3)	4437.43(17)	19875.7(19)	3370.1(2)
Z	4	4	8	4
μ/mm^{-1}	7.199	6.806	6.013	8.86
Reflections collected/independent	34614, 20837	43213, 9761	24887, 12866	24580, 3864
$R1$, $wR2$ [$I > 2\sigma(I)$]	0.057, 0.130	0.045, 0.125	0.110, 0.235	0.064, 0.146

[a] The data were of low quality and only a partial structure was obtained.

Crystal structure determinations

Data were collected using a Nonius Kappa-CCD diffractometer using COLLECT (Nonius, 1998) software, with $\lambda = 0.71073$ Å. The unit cell parameters were calculated and refined from the full data set. Crystal cell refinement and data reduction were carried out using the Nonius DENZO package. The data were scaled using SCALEPACK (Nonius, 1998) and no other absorption corrections were applied. Friedel pairs were kept separate. The SHELXTL 5.1 program package[19] was used to solve the structure by direct methods, followed by refinement using successive difference Fourier syntheses.

Crystals of $[Au_4(\mu\text{-}Ph_2PCH_2PPh_2)_2(\mu\text{-}NC_5H_4C_5H_4N)_2][CF_3CO_2]_4\cdot CH_2Cl_2$ were grown by slow diffusion of pentane into a methylene chloride solution. A white wedge shaped crystal was mounted on a glass fiber. The cation was refined anisotropically except for the phenyl rings which were also constrained to be regular hexagons (AFIX 66). Of the four anions, two refined well anisotropically but the other two were disordered (modeled as 60/40 and 50/50 abundance), and the geometries were constrained to be the same. The CH_2Cl_2 molecule of solvation was disordered also (50/50 abundance) and the C–Cl (1.65 Å) and the Cl · · · Cl (2.74 Å) distances were fixed and the atoms kept isotropic. The crystal was twinned and the BASF parameter refined to a value of 0.500.

Crystals of $[(\mu\text{-}Ph_2P(CH_2)_3PPh_2)Au(\mu\text{-}NC_5H_4C_5H_4N)Au]_2[CO_2CF_3]_4\cdot CH_2Cl_2\cdot C_5H_{12}$ were grown similarly. A pale yellow cube was mounted on a glass fiber. All of the non-hydrogen atoms in the cation were refined with anisotropic thermal parameters. One of the crystallographically distinct trifluoroacetate anions was well behaved but the other was disordered and modeled as two units in a 60/40 mix. The 60% model was refined anisotropically and the 40% model isotropically, with fixed geometry. The molecules of solvation were refined at half occupancy.

Crystals of $[Au_4(\mu\text{-}Ph_2P(CH_2)_5PPh_2)_2(\mu\text{-}NC_5H_4C_5H_4N)_2][CF_3CO_2]_4$ were grown similarly. A colorless needle was cut and the resulting block mounted on a glass fiber. The crystal was of poor quality and several constraints were needed, such that the structure was only of sufficient quality to determine the overall geometry. The pyridyl groups were constrained to be flat, phenyl groups to be hexagons (AFIX 66); the $P(CH_2)_5P$ group to have P–C 1.85, C–C 1.54 Å and the geometry of the trifluoroacetate anions was fixed. The atoms Au4, P4 and C10 were disordered over two positions and refined isotropically, while Au1, Au2, Au3, P1, P2, P3, and C1–C9 were anisotropic. The crystal was twinned and the BASF factor refined to a value of 0.294.

Crystals of $[(CF_3CO_2)Au(\mu\text{-}Ph_2P(CH_2)_4PPh_2)Au(O_2CCF_3)]$ were grown from dichloromethane–pentane. A tiny, colorless needle was mounted on a glass fibre. All non-hydrogen atoms were refined with anisotropic thermal parameters. Crystal data are given in Table 8.

CCDC reference number 186/2237.

Acknowledgements

We thank the NSERC (Canada) for financial support to R. J. P. and for a scholarship to M.-C. B.

References

1 D. M. P. Mingos and R. P. F. Kanter, *J. Organomet. Chem.*, 1990, **384**, 405; G. Jia, R. J. Puddephatt, J. D. Scott and J. J. Vittal, *Organometallics.*, 1993, **12**, 3565; S.-J. Shieh, X. Hong, S.-M. Peng and C.-M Che, *J. Chem. Soc.*, *Dalton Trans.*, 1994, 3067; P. M. Van Calcar, M. M. Olmstead and A. L. Balch, *J. Chem. Soc.*, *Chem. Commun.*, 1995, 1773; M. J. Irwin, G. Jia, N. C. Payne and R. J. Puddephatt, *Organometallics*, 1996, **15**, 51; M. J. Irwin, L. M. Muir, K. W. Muir and R. J. Puddephatt, *Chem. Commun.*, 1997, 219.
2 S. S. Pathameni and G. R. Desiraju, *J. Chem. Soc.*, *Dalton Trans.*, 1993, 319.
3 J. J. Guy, P. G. Jones, M. J. Mays and G. M. Sheldrick, *J. Chem. Soc.*, *Dalton Trans.*, 1977, 8.
4 P. G. Jones, G. M. Sheldrick and E. Hadicke, *Acta Crystallogr.*, *Sect. B*, 1980, **36**, 2777.
5 K. P. Hall and D. M. P. Mingos, *Inorg. Chem.*, 1984, **22**, 237.
6 Y. Jiang, S. Alvarez and R. Hoffmann, *Inorg. Chem.*, 1985, **24**, 749.
7 N. Rosch, A. Gorling, D. E. Ellis and H. Schmidbaur, *Angew. Chem.*, *Int. Ed. Engl.*, 1989, **28**, 1357; H. Schmidbaur, W. Graf and G. Müller, *Angew. Chem.*, *Int. Ed. Engl.*, 1988, **27**, 417.
8 P. M. Van Calcar, M. M. Olmstead and A. L. Balch, *Inorg. Chem.*, 1997, **36**, 5231.
9 (*a*) M. J. Irwin, J. J. Vittal, G. P. A. Yap and R. J. Puddephatt, *J. Am. Chem. Soc.*, 1996, **118**, 13101; (*b*) R. J. Puddephatt, *Chem. Commun.*, 1998, 1055; (*c*) M. J. Irwin, L. M. Rendina, J. J. Vittal and R. J. Puddephatt, *Chem. Commun.*, 1996, 1281.
10 A. Tamaki and J. K. Kochi, *J. Organomet. Chem.*, 1974, **64**, 411.
11 I. J. B. Lin, J. M. Hwang, D.-F. Feng, M. C. Cheng and Y. Wang, *Inorg. Chem.*, 1994, **33**, 3467.
12 H. Schmidbaur, A. Wohlleben, F. Wagner, O. Orama and G. Huttner, *Chem. Ber.*, 1997, **110**, 1748.
13 P. A. Bates and J. M. Waters, *Inorg. Chim. Acta*, 1985, **98**, 125.
14 D. F. Chodosh, D. S. Eggleston, G. R. Girard and D. T. Hill, *Inorg. Chim. Acta*, 1985, **108**, 221.
15 M. K. Cooper, K. Hendrick, M. L. McPartlin, E. Mitchell and A. Scott, *Inorg. Chim. Acta*, 1984, **84**, L9.
16 A. Sarkar and S. Chakravorti, *J. Lumin.*, 1995, **65**, 163; D. Li, X. Hong, C.-M. Che, W.-C. Lo and S.-M. Peng, *J. Chem. Soc.*, *Dalton Trans.*, 1993, 2929.
17 L. Hao, R. J. Lachicotte, H. J. Gysling and R. Eisenberg, *Inorg. Chem.*, 1999, **38**, 4616; V. W. W. Yam and K. K. W. Lo, *Chem. Soc. Rev.*, 1999, **28**, 323; J. M. Forward, D. Bohmann, J. P. Fackler, Jr. and R. J. Staples, *Inorg. Chem.*, 1995, **34**, 6330; W. B. Jones, J. Yuan, R. Narayanaswamy, M. A. Young, R. C. Elder, A. E. Bruce and M. R. M. Bruce, *Inorg. Chem.*, 1995, **34**, 1996.
18 CAChe Scientific 3.7, Molecular Mechanics, Conjugated Gradients, Oxford Molecular Group, Oxford, 1994.
19 G. M. Sheldrick, SHELXTL, version 5.1, Siemens Analytical X-Ray instruments, Madison, WI, 1998.